

SUBTIDAL WAVE PROPAGATION IN TAMPA BAY

By

KIRSTEN NIELSEN

A THESIS PRESENTED TO THE GRADUATE SCHOOL  
OF THE UNIVERSITY OF FLORIDA IN PARTIAL FULFILLMENT  
OF THE REQUIREMENTS FOR THE DEGREE OF  
MASTER OF SCIENCE

UNIVERSITY OF FLORIDA

2014

© 2014 Kirsten Nielsen

To Matthew

## ACKNOWLEDGMENTS

I would first like to thank my committee, Arnolando Valle-Levinson and Maitane Olabarrieta, for being supportive and helpful through this process. I would also like to thank my research group for providing useful input and assisting me throughout my research. Without both parties, I would not have produced the following thesis. Finally, I would like to thank my husband, Matthew, for always believing in me.

## TABLE OF CONTENTS

	<u>page</u>
ACKNOWLEDGMENTS.....	4
LIST OF FIGURES.....	6
LIST OF ABBREVIATIONS.....	7
ABSTRACT .....	9
CHAPTER	
1 INTRODUCTION .....	11
Motivation .....	11
Storm Surge.....	11
2 METHODS.....	12
Study Area .....	12
Data Collection .....	13
Data Analysis.....	14
The Model.....	15
3 RESULTS .....	20
Subtidal Water Levels and Meteorological Data .....	20
Wavelet Analysis .....	21
CEOF Analysis .....	21
4 DISCUSSION .....	34
5 CONCLUSION.....	39
LIST OF REFERENCES .....	40
BIOGRAPHICAL SKETCH.....	41

## LIST OF FIGURES

<u>Figure</u>	<u>page</u>
2-1 Divisions of Tampa Bay .....	18
2-2 Station Locations for Data Collection.....	19
3-1 Tidal and Subtidal Water Levels at McKay Bay .....	23
3-2 Tidal and Subtidal Water Levels at Old Port Tampa.....	24
3-3 Tidal and Subtidal Water Levels at Port Manatee.....	25
3-4 Tidal and Subtidal Water Levels at St Petersburg .....	26
3-5 Subtidal water levels at each port in 2012 .....	27
3-6 Atmospheric pressure at Old Port Tampa .....	28
3-7 Wind speed and direction at Old Port Tampa .....	29
3-8 Morlet Wavelet power spectrum for subtidal water level.....	30
3-9 Time Series of EOF Modes 1 and 2 .....	31
3-10 Amplitude of Mode 1.....	32
3-11 Phase of Mode 1 .....	33
4-1 Ideal basin bathymetry .....	36
4-2 RMSe of various $\kappa$ and $\delta$ values .....	37
4-3 Amplitude comparison between Mode 1 and values from the model.....	38

## LIST OF ABBREVIATIONS

$\frac{\partial u}{\partial x}$	Velocity gradient
$\frac{\partial u}{\partial t}$	Local acceleration
$\frac{\partial \eta}{\partial x}$	Water surface gradient
$A_z$	Eddy viscosity
$B'$	Half the basin width
$C'$	Wave celerity
CEOF	Complex empirical orthogonal functions
EOF	Empirical orthogonal functions
$f'$	Coriolis acceleration
$g'$	Gravitational acceleration
$H'$	Water depth
$h$	Non-dimensional depth
$L'$	Length of basin
$M_0$	Complex function of $f$ , $\delta$ , and $h$
$N_0$	Sea level
NOAA	National Oceanographic and Atmospheric Administration
PORTS	Physical Oceanographic Real-Time System
$P_0$	Complex function of $f$ , $\delta$ , and $h$
$Q_0$	Complex function of $f$ , $\delta$ , and $h$
Re[ ]	Real part of the function
$t$	Time
$u$	Velocity of flow

$u_0$	Complex velocity amplitude
$U(z)$	Velocity of flow as a function of depth
$x$	Non-dimensional distance along basin
$y$	Non-dimensional distance across basin with center origin
$z$	Non-dimensional depth of the basin
$\alpha$	Aspect ratio of the basin
$\eta$	Water surface
$\kappa$	Geometric parameter
$\mu$	Frictional parameter
$\epsilon$	Ratio of the amplitude of the wave at the open end to the maximum depth

Abstract of Thesis Presented to the Graduate School  
of the University of Florida in Partial Fulfillment of the  
Requirements for the Degree of Master of Science

## SUBTIDAL WAVE PROPAGATION IN TAMPA BAY

By

Kirsten Nielsen

May 2014

Chair: Arnaldo Valle-Levinson

Major: Coastal and Oceanographic Engineering

Hourly water level data were obtained from four locations in Tampa Bay for the year 2012. These data were low pass filtered to retain the subtidal water levels. Atmospheric pressure and wind data were taken at Old Port Tampa in hourly intervals to help explain the maximum in subtidal water level. A Morlet wavelet transform on the subtidal water level found high energy during the maximum water level in 4-16 day period band. To further analyze the subtidal water level data, Complex Empirical Orthogonal Functions of the subtidal water level were found in order to gain understanding on temporal and spatial variability of the subtidal wave propagation. The amplitude of mode 1 increased between Port Manatee and Old Port Tampa and decreased between Old Port Tampa and McKay Bay. These amplifications and attenuation of the subtidal signal correspond to the geography of the bay and the locations of the ports. The phase of the signal was nearly  $0^\circ$  through the bay, indicative of a standing wave. Finally, an analytical model for a frictional wave was used to gain more information of the dynamics of these pulses in the bay. Values of  $\kappa$ , a measure of wavelength to basin length, and  $\delta$ , a frictional damping parameter, were varied in order to match the amplitude of mode 1. The best fit values for  $\kappa$  and  $\delta$  explained that the

length of the basin is approximately one-tenth the wavelength of the subtidal pulse and friction influenced the entire water column.

## CHAPTER 1 INTRODUCTION

### **Motivation**

For coastal communities around the world, storm surge is a major threat to both life and property. Understanding how storm surge and other subtidal waves propagate through coastal environments is crucial for reducing and possibly preventing any damage to the community. Various studies have surfaced through recent years due to increased awareness of the destruction caused by storm surge.

### **Storm Surge**

Recent history has shown the impact storm surge can make with a large storm. In 2004, Hurricane Katrina caused a great deal of devastation by inundating New Orleans. The combination of the low elevation of the city (below sea level), the failure of levies and the storm's speed caused complete destruction in the city and surrounding areas. Since this event, there has been an increase in studies into storm surge in varying environments. Some wish to better model the impending storm surge in hopes to better predict in the future. For example, one study focused on the northeastern part of the United States [*Sheng et al.*, 2010]. This research used a simulation to predict the damage caused by severe storms. Other studies focus on other environmental factors and their interaction with storm surge, such as sea level rise [*Tebaldi et al.*, 2012].

## CHAPTER 2 METHODS

### Study Area

This study takes place in Tampa Bay in Florida. Tampa Bay is the largest open water estuary in Florida and acts as a major port to the area. The bay is divided into four major subsections: Old Tampa Bay, Hillsborough Bay, Middle Tampa Bay and Lower Tampa Bay [Lewis and Estevez, 1988]. The area studied in this analysis is Hillsborough Bay, Middle Tampa Bay and Lower Tampa Bay shown in Figure 2-1. In this area, the bay length is approximately 50 km and the width is 15 km. The bay is shallow at an area-weighted depth of 4 m [Galperin et al., 1991] but is as deep as 25 m (near Edgemont Key) in the dredged shipping channel (mainly 15m throughout the shipping channel). The volume of the bay is approximately  $4 \times 10^9 \text{ m}^3$ . The surrounding watershed includes Pinellas, Hillsborough, Manatee, Pasco, Sarasota, and Polk counties and the surface area of the bay with the water shed is  $4600 \text{ m}^3$  [Weisberg and Zheng, 2006]. The flow of fresh water into the bay (annual flow rate of  $63 \text{ m}^3 \text{ s}^{-1}$ ) comes from the Hillsborough, Alafia, Little Manatee and Manatee rivers (as well as some smaller streams, springs and land drainage).

The period of oscillation, given by Merian's formula, was determined using the following formula.

$$T = \frac{4L}{\sqrt{gh}} \quad (2-1)$$

T is the period of oscillation, L is the length of the bay, g is the gravitational acceleration and h is the approximate constant depth. The period of oscillation for Tampa Bay is heavily dependent on the depth which varies in different locations. For

the area weighted depth of 4 m, the period of oscillation is 8.9 hours. For the maximum depth of 25 m, the period of oscillation is 3.5 hours.

The tidal forcing in Tampa Bay is mixed but dominated by  $M_2$  and  $O_1$  astronomic constituents [Goodwin 1987]. The periods of these tides are 12.421hr and 25.82 hr respectively [Mellor 1996]. The tidal range has temporal variability but the average tidal range is 0.7 m. The tidal current amplitude decreases as it travels through the bay, starting at 1.2-1.8  $\text{ms}^{-1}$  at the mouth to 0.15  $\text{ms}^{-1}$  in Hillsborough Bay. The flood tide takes about 3.5 hours to traverse the entire bay from mouth to ends of Old Tampa Bay and Hillsborough Bay. The maximum ebb velocities are greater than the maximum flood velocities.

The Tampa Bay climate is subtropical with long, warm, humid summers and dry, mild winters. The annual rainfall is about 1.35 m which primarily takes place during June and September [Lewis and Estevez 1988]. The period of extensive rainfall coincides with hurricane season. The tropical cyclones typically enter the region from the southeast to the southwest and move north.

### **Data Collection**

The variable of interest in this study was water level. Other variables affecting water level, such as wind velocity and pressure, were not initially considered. However, an unexplained maximum in the subtidal water level results required further information in order to discover the reason for this extraneous result. The data used in conjunction with the subtidal water level were atmospheric pressure and wind velocity and direction. The data were gathered using the Physical Oceanographic Real-Time System (PORTS) offered by the National Ocean Service of the National Oceanic and Atmospheric Administration (NOAA). This program gives real-time oceanographic data at various

locations across the US. For this study, the location chosen was Tampa Bay in Florida. The data were collected from four stations within Tampa Bay: Port Manatee, St. Petersburg, Old Port Tampa, and McKay Bay. The locations of these ports are shown in Figure 2-2.

The water level data collected from these stations were at 1 hr intervals from January 1<sup>st</sup>, 2012 to December 31<sup>st</sup>, 2012. All data were measured in reference to the mean sea level datum and Greenwich Mean Time. Water level data were measured in meters, pressure data were measure in millibars, wind speed was measured in meters per second and wind direction was measured in degrees.

### **Data Analysis**

The data were then low pass filtered at 40 hours with a Lanczos filter. At this point, the subtidal water levels were examined. After examination, pressure and wind data were also examined in conjunction with the water level data. The water level data were also analyzed using the wavelet transform. The wavelet transform will “find the dominant modes of variability and how those modes vary in time” [Torrence and Compo, 1998] in the subtidal water level.

For the statistical analysis, the Hilbert transform was applied to the subtidal water level data. This converted each signal to a time series of complex numbers. This new time series result in the real part of the complex number to remain as the original signal and the complex part to be the original signal shifted by 90°. This also resulted in the real part being independent or orthogonal to the imaginary part. This transform was done in order to find the phase propagation information from station to station. This is found by using Complex Empirical Orthogonal Functions (CEOFs). Finding the CEOF functions means solving the eigenvalue problem related to the covariance of the

transformed (complex) matrix of data. The CEOF functions gave spatial and temporal information based on the subtidal water level.

### The Model

*Winant* [2007] created a linear analytical model for flow in an elongated basin with the stipulation that the basin width is smaller than the Rossby radius. This model also uses constant vertical eddy diffusivity. Based on the assumptions, the model was derived from the continuity equation and momentum balance. To solve these equations, non-dimensional variables were developed.

$$\frac{\partial u}{\partial x} + \frac{\partial v}{\partial y} + \frac{\partial w}{\partial z} = 0 \quad (2-2)$$

$$\frac{\partial u}{\partial t} - fv = -g \frac{\partial \eta}{\partial x} + \frac{\partial}{\partial z} \left[ A_z \frac{\partial u}{\partial z} \right] \quad (2-3)$$

$$\frac{\partial v}{\partial t} + fu = -g \frac{\partial \eta}{\partial y} + \frac{\partial}{\partial z} \left[ A_z \frac{\partial v}{\partial z} \right] \quad (2-4)$$

$$u = \frac{u'}{\epsilon \omega' L'} \quad (2-5)$$

$$v = \frac{v'}{\epsilon \omega' B'} \quad (2-6)$$

$$w = \frac{w'}{\epsilon \omega' H'} \quad (2-7)$$

$$\eta = \frac{\eta'}{C'} \quad (2-8)$$

$$\alpha = \frac{B'}{L'} \quad (2-9)$$

$$\kappa = \frac{\omega' L'}{\sqrt{g' H'}} \quad (2-10)$$

$$\delta = \sqrt{\frac{2A_z'}{\omega' H'^2}} \quad (2-11)$$

$$f = \frac{f'}{\omega'} \quad (2-12)$$

$$t = \omega' t' \quad (2-13)$$

$$x = \frac{x'}{L'} \quad (2-14)$$

$$y = \frac{y'}{B'} \quad (2-15)$$

$$(z, h) = \frac{(z' h')}{H'} \quad (2-16)$$

Each variable with a ' signifies the dimensional value.  $\omega'$  is motion frequency,  $L'$  is the length of the basin,  $2B'$  is maximum width of the basin,  $H'$  is maximum basin depth,  $\eta'$  is the free surface elevation,  $C'$  is the wave celerity,  $g'$  is the gravitational acceleration,  $A_z'$  is the eddy viscosity,  $f'$  is the Coriolis parameter,  $x'$  is the direction along the basin where  $x'=0$  is at the entrance of the basin,  $y'$  is the direction across the basin where  $y'=0$  is in the middle of the basin. and  $z'$  is the positive direction out of the basin where  $z'=0$  is on the undisturbed free surface. The non dimensional variables of significance are  $\epsilon$ ,  $\alpha$ ,  $\kappa$ , and  $\delta$ .  $\epsilon$  is the ratio of the amplitude of the wave at the open end to the maximum depth such that the water surface is located at  $z = \epsilon\eta$ .  $\alpha$  is the horizontal aspect ratio of the basin,  $\delta$  measures the relative importance of friction to local acceleration, and  $\kappa$  is the relative measure of the length of the basin to the wavelength. Substituting the non dimensional variables into the momentum balance equations yields the following equations.

$$\frac{\partial u}{\partial x} + \frac{\partial v}{\partial y} + \frac{\partial w}{\partial z} = 0 \quad (2-16)$$

$$\frac{\partial u}{\partial t} - f\alpha v = -\frac{1}{\kappa^2} \frac{\partial \eta}{\partial x} + \frac{\delta^2 \partial^2 u}{2\partial z^2} \quad (2-17)$$

$$\frac{\partial v}{\partial t} + \frac{f}{\alpha} u = -\frac{1}{\alpha^2 \kappa^2} \frac{\partial \eta}{\partial y} + \frac{\delta^2 \partial^2 v}{2\partial z^2} \quad (2-18)$$

Solutions for the along estuary, cross estuary, and vertical velocity amplitudes and the water level amplitude are given below.

$$u = \text{Re}[U(z)e^{-i\omega t}] \quad (2-19)$$

$$v = \text{Re}[V(z)e^{-i\omega t}] \quad (2-20)$$

$$w = \text{Re}[W(z)e^{-i\omega t}] \quad (2-21)$$

$$\eta = \text{Re}[N(z)e^{-i\omega t}] \quad (2-22)$$

This study focused on the free surface elevation, therefore the significant variable is N. The assumption that the depth varied solely across the basin (y direction) led to using the lowest order solution for N. At the entrance of the basin (x=0), N is assumed to be 1.

$$N = \frac{\cos[\kappa\mu(1-x)]}{\cos[\kappa\mu]} \quad (2-23)$$

$$\mu = \langle M_0 \rangle^{-1/2} \quad (2-24)$$

$$\langle M_0 \rangle = \int_0^1 M_0 dy \quad (2-25)$$

The variable  $\mu$  represents the frictional behavior of the basin. The variable of interest, N, gives the amplitude of a subtidal wave through the basin. The value depends largely on the parameters  $\kappa$  and  $\delta$ .  $\kappa$  (Equation 2-10) compares the length of the basin to the length of the wave being studied. The value of  $\delta$  signifies the importance of the friction throughout the water column. The lower values of  $\delta$  ( $\delta < 1$ ) relate to a lower friction system while higher values of  $\delta$  ( $\delta > 1$ ) represent a high friction system impacting local accelerations. The analytical results from the model were compared to the CEOF analysis and the  $\kappa$  and  $\delta$  parameters were altered to find the best fit for the data.

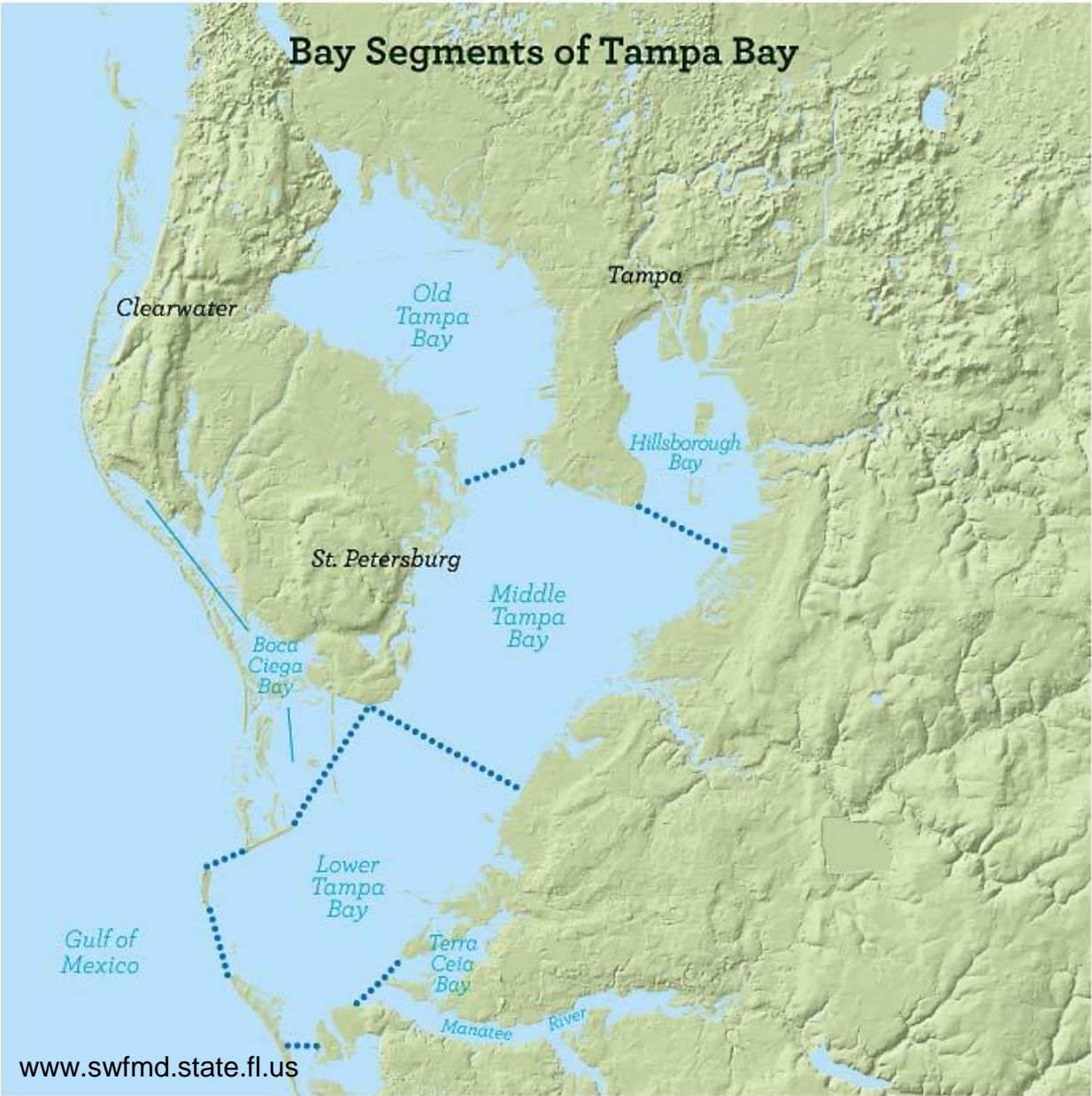


Figure 2-1. Divisions of Tampa Bay (Available online from [www.swfmd.fl.us](http://www.swfmd.fl.us))

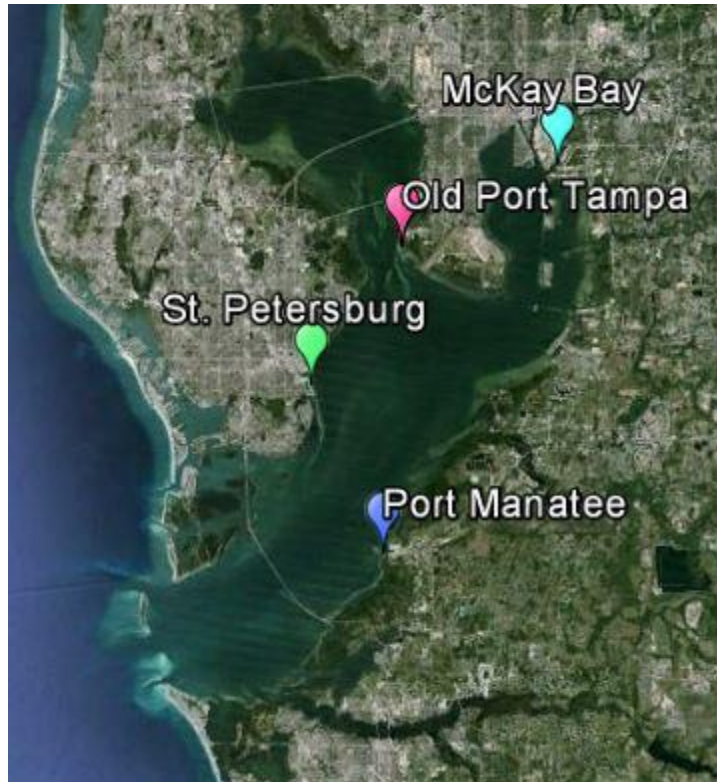


Figure 2-2. Station Locations for Data Collection (Available from Google Earth)

## CHAPTER 3 RESULTS

### **Subtidal Water Levels and Meteorological Data**

The subtidal water levels for each station are shown in Figure 3-1 (McKay Bay), Figure 3-2 (Old Port Tampa), Figure 3-3 (Port Manatee), and Figure 3-4 (St Petersburg). The combined plot shown in Figure 3-5 shows a few interesting facts about the water levels at the various stations. The first half of the year shows absolute minimum water levels in the bay at Old Port Tampa. The second half of the year shows absolute minimum water levels at McKay Bay. Also, the second half of the year shows increased variability of the subtidal water levels, commonly changing between approximately -0.2 meters to 0.4 meters. Finally, there is an absolute maximum water level at each station in late April. This maximum is close to 1 meter, which is significantly larger than surrounding local maxima. To investigate possible reasons behind these phenomena, pressure and wind data were processed.

Both pressure and wind data were also taken at hourly intervals throughout the year of 2012. Due to a limited number of stations offering this particular type of meteorological data, both the wind data and pressure data were taken from Old Port Tampa.

The pressure at Old Port Tampa (Figure 3-6) had minima in late April, late June and late October. The minimum in late April coincided with the maximum subtidal water level and is likely the reason behind this maximum. The wind at Old Port Tampa (Figure 3-7) showed winds from the northwest during the water level maximum in late April. The other instances of winds from the northwest occurred with periods of variability. The wind impacted both the overall maximum water level and the periods of variability.

## **Wavelet Analysis**

In order to further investigate the reasoning behind the phenomena seen in the subtidal water level data, the data were analyzed using the wavelet transform. Wavelet analysis offers information on the dominant modes of variability and how it varies in time. This differs from a spectrum which assumes a stationary signal. A Morlet wavelet transform (MWT) was used on the subtidal water level and the resulting wavelet coherence is shown in Figure 3-8. A cone of influence is included in the plot in order to exclude results with no statistical reliability. A continuous wavelet transform tends to have increased error at the edges of the data. The maximum energy in the wavelet is shown in late April and early May. This high power occurs in the 4-16 day period band. Due to the timing of this high energy, it is likely due to the maximum water level incident seen in the subtidal data sets. Other peaks in power occur in late June and late October. These periods of time coincide with local maximums and minimums in the subtidal water level. These high energies also relate to lows in pressure.

## **CEOF Analysis**

The subtidal water level data were then analyzed using CEOFs in order to explain the temporal and spatial variability of the pulses. The temporal variability (Figure 3-9) is primarily explained by the first mode with mode 1 holding 97% of the variance. The time series portrays this result by showing the little variation in mode 2. The majority of oscillation in mode 2 is seen in the second half of the year. Even with the greater oscillation, however, the amplitude stays close to zero. For this reason, only mode 1 is examined for these results. The spatial variability (Figure 3-10) shows an amplification of the signal from Port Manatee to St Petersburg (4% amplification) and from St Petersburg to Old Port Tampa (11% amplification) while decreasing between

Old Port Tampa and McKay Bay (2% attenuation). The amplification of the signal grows as the wave travels through the bay. The decrease in the signal results from the location of the McKay Bay station. Looking back at Figure 2-2, the McKay Bay station is well protected from the point of entry into Tampa Bay. The other stations have limited obstructions between their respective locations and the incoming wave path. McKay Bay must be influenced by diffracted and reflected waves. Therefore, the attenuation of the amplitude is explained by the geometry of the bay. The phase of the subtidal wave varied from  $-1.8^\circ$  to  $0^\circ$  (nearly zero throughout the bay). This near zero phase change throughout the bay suggests the behavior of a standing wave.

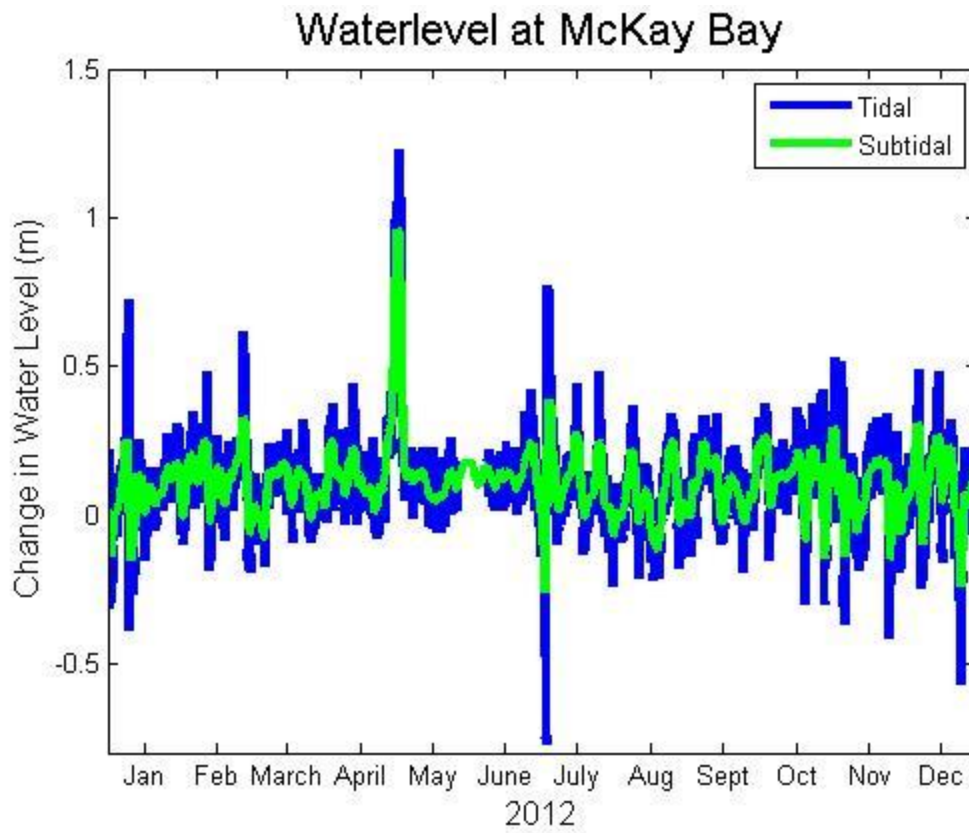


Figure 3-1. Tidal and Subtidal Water Levels at McKay Bay

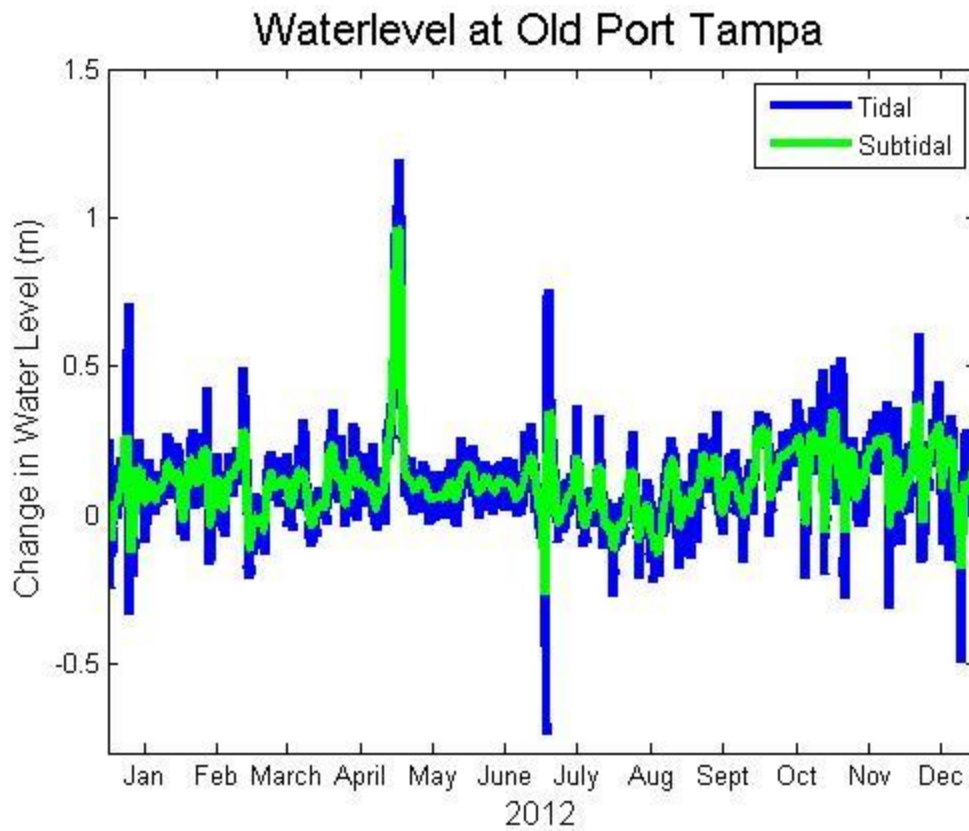


Figure 3-2. Tidal and Subtidal Water Levels at Old Port Tampa

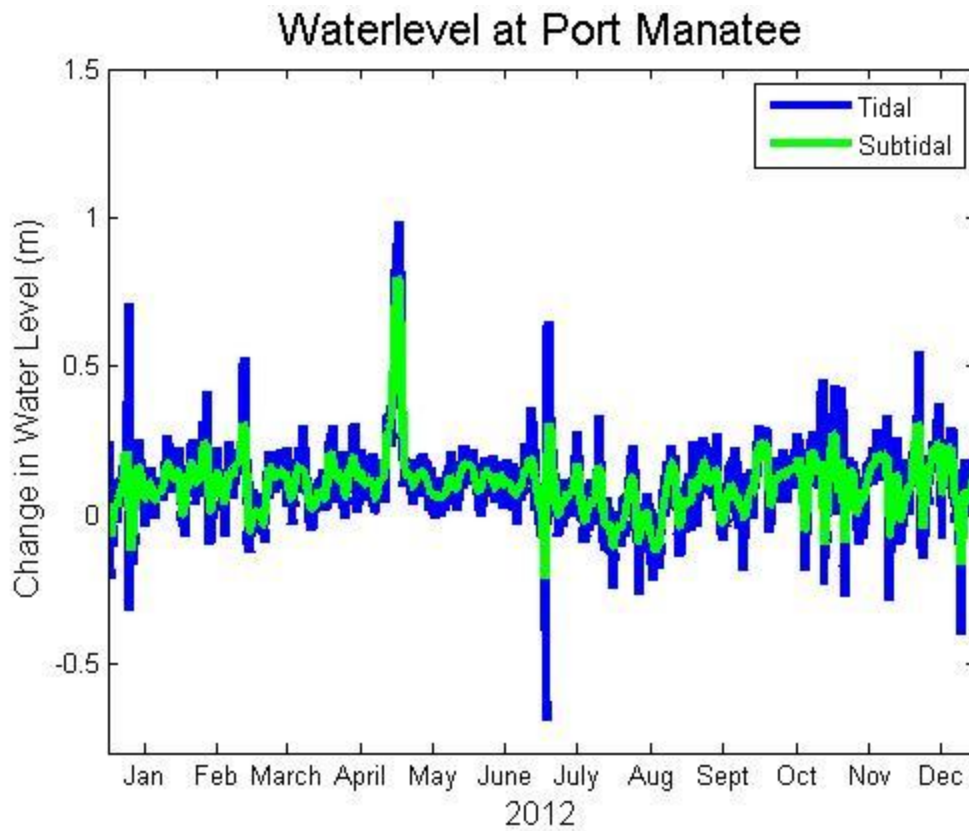


Figure 3-3. Tidal and Subtidal Water Levels at Port Manatee

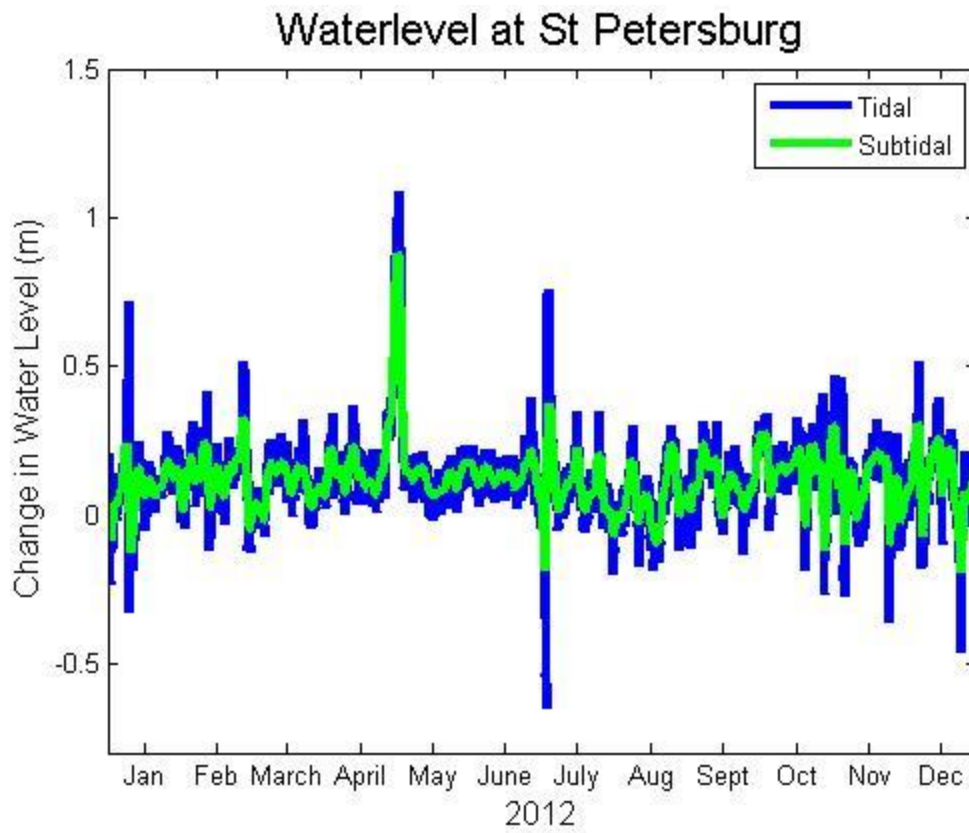


Figure 3-4. Tidal and Subtidal Water Levels at St Petersburg

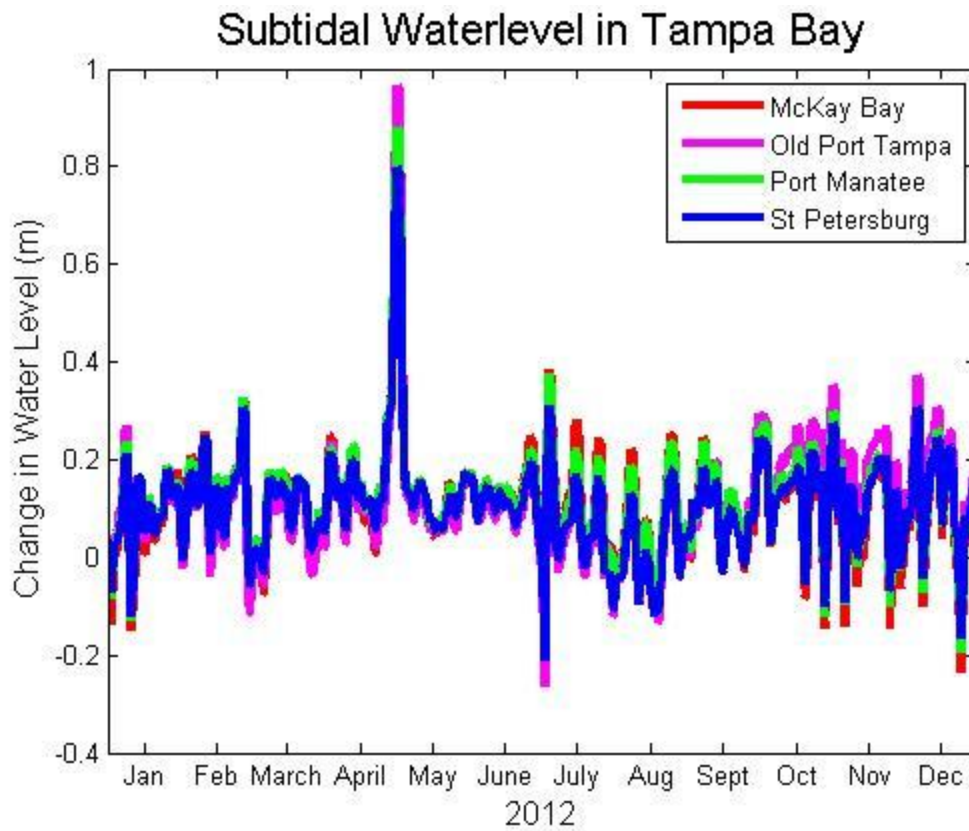


Figure 3-5. Subtidal water levels at each port in 2012

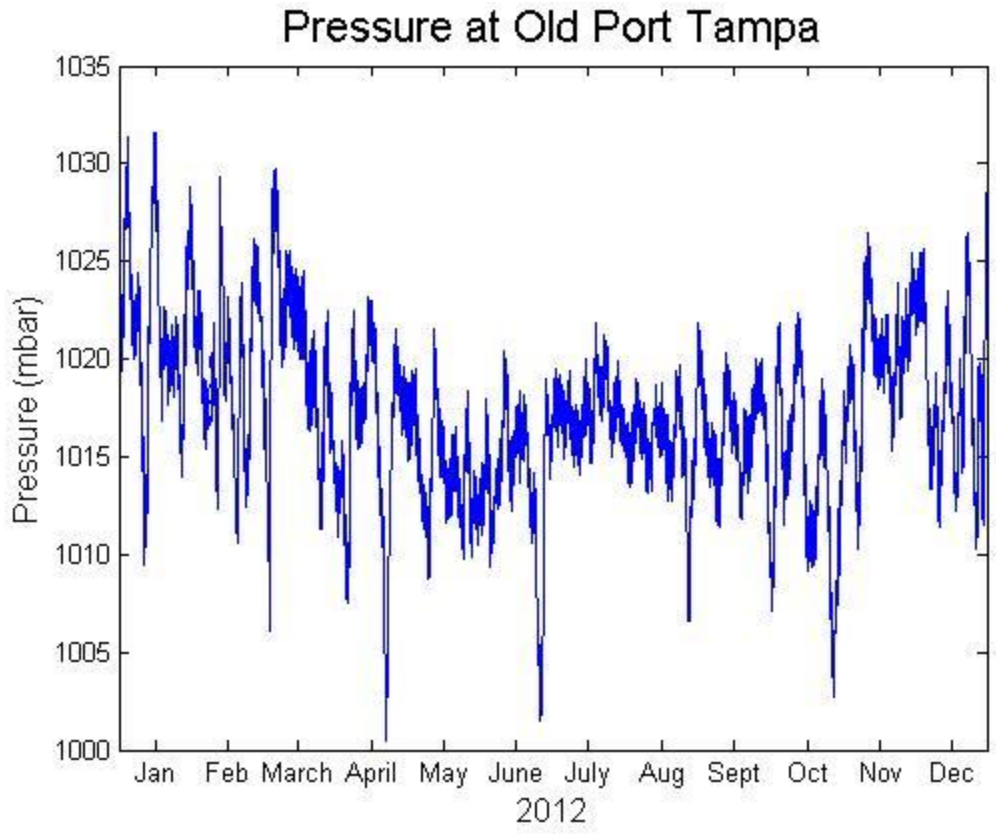


Figure 3-6. Atmospheric pressure at Old Port Tampa

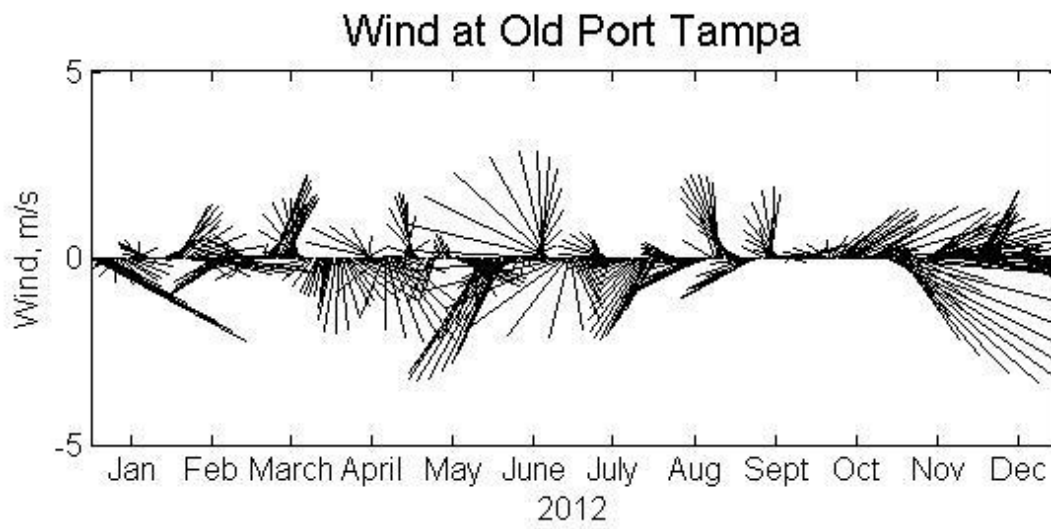


Figure 3-7. Wind speed and direction at Old Port Tampa

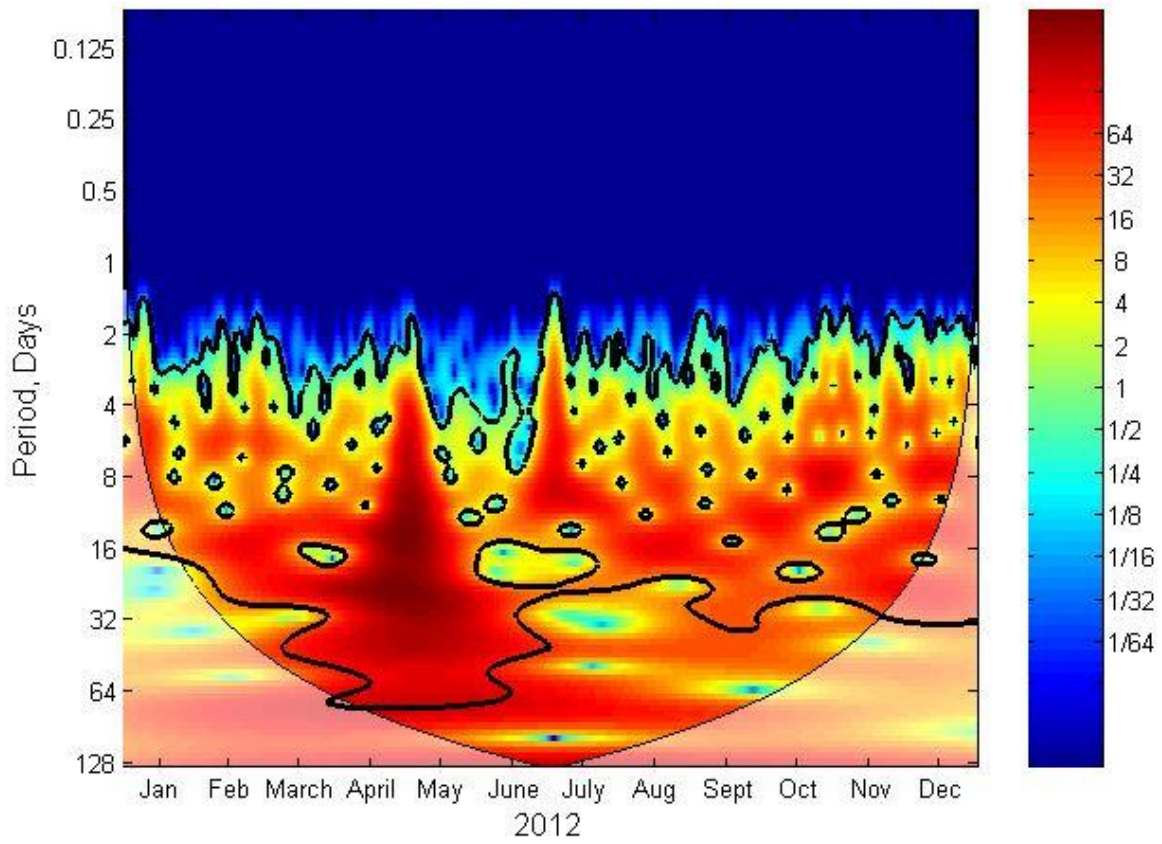


Figure 3-8. Morlet Wavelet power spectrum for subtidal water level

### Time Series of EOFs

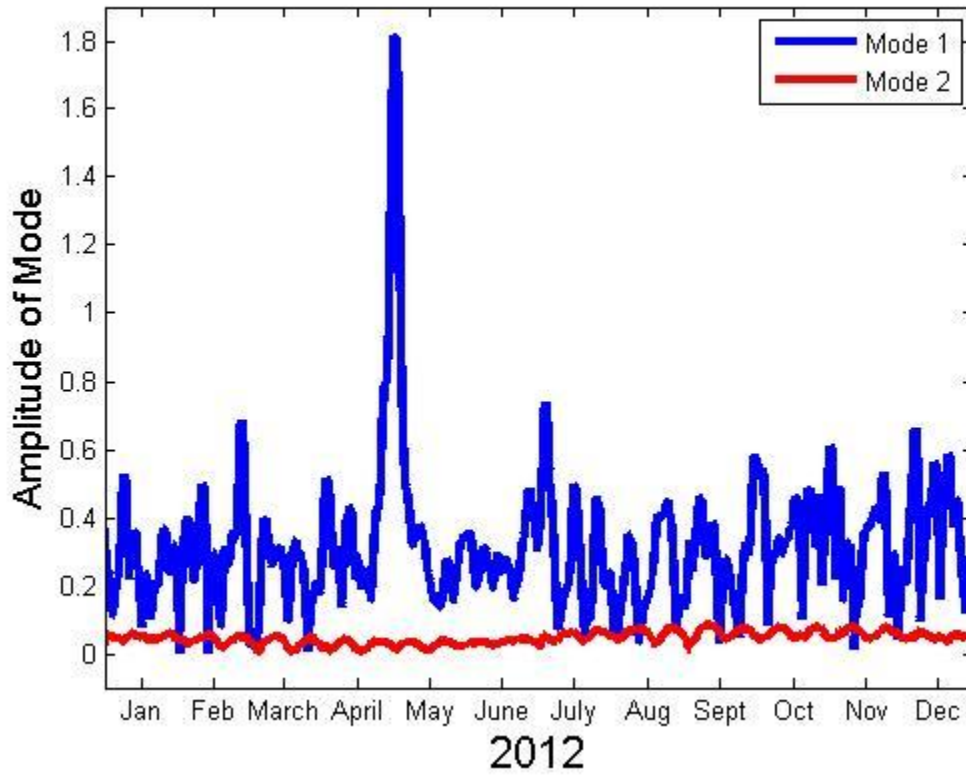


Figure 3-9. Time Series of EOF Modes 1 and 2

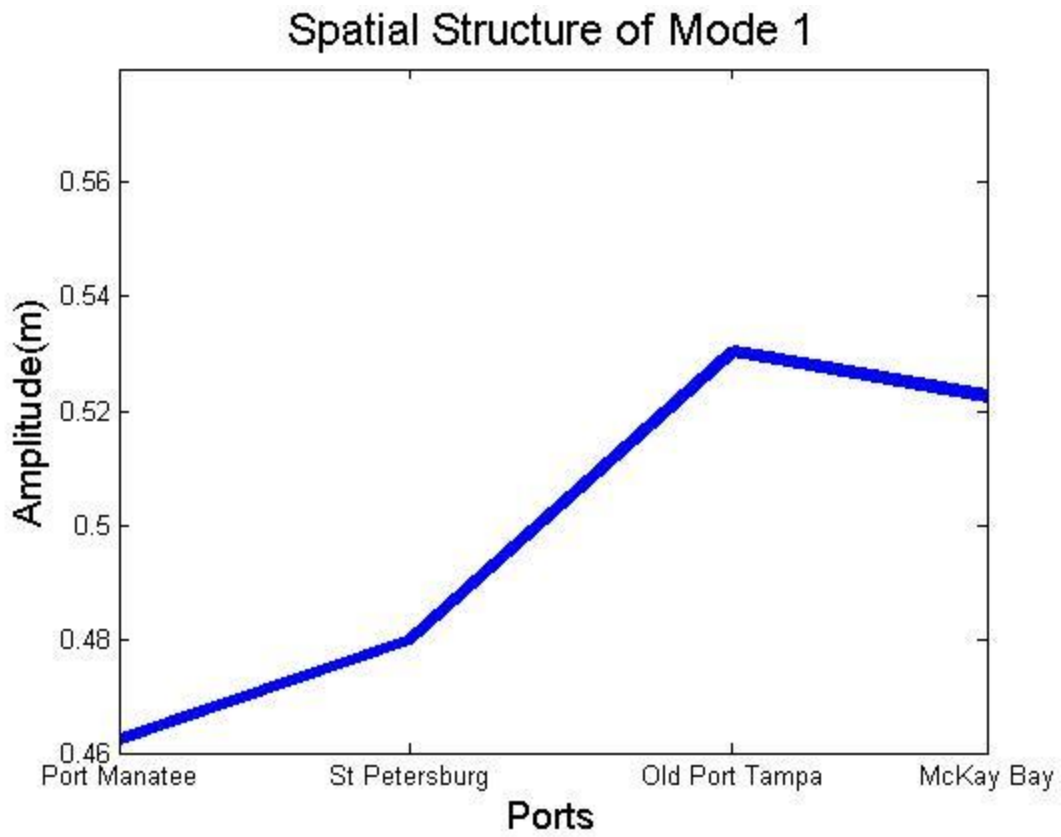


Figure 3-10. Amplitude of Mode 1

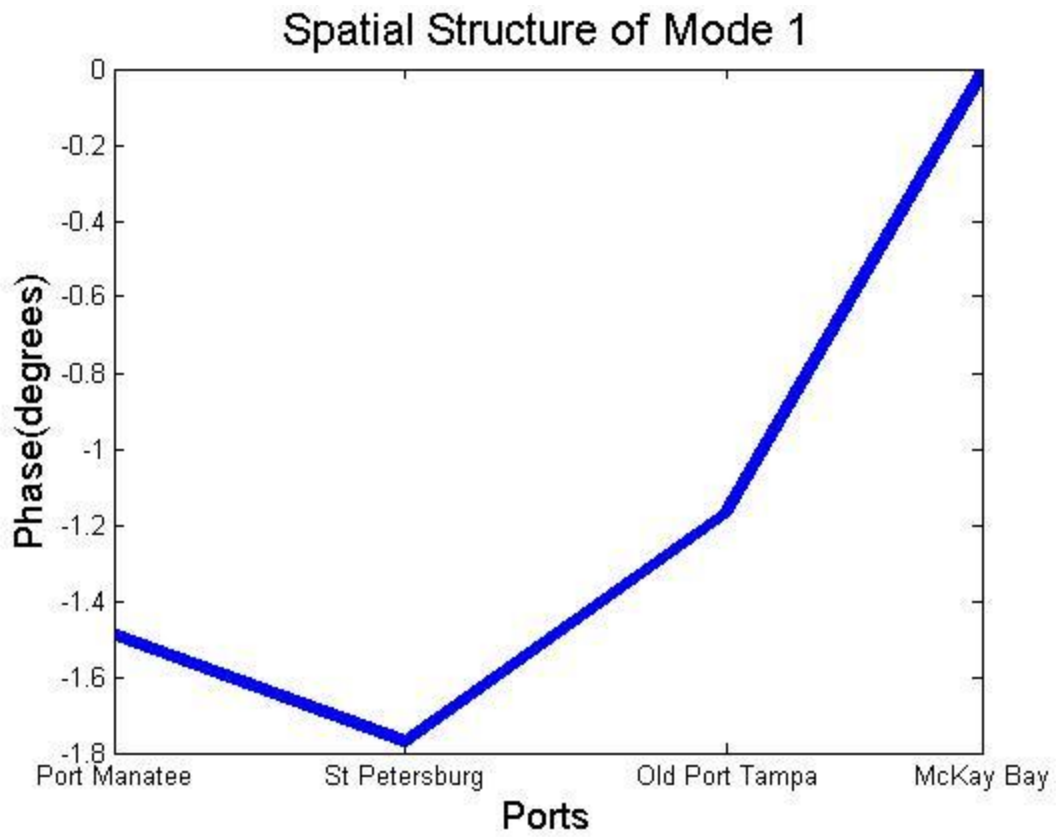


Figure 3-11. Phase of Mode 1

## CHAPTER 4 DISCUSSION

The behavior of subtidal wave propagation in Tampa Bay was defined by comparing the CEOF results to the results of the analytical model. The model, proposed by *Winant* [2007], is used to describe the motion of a long wave through a basin by balancing the pressure gradient with frictional effects. The model can be used to solve for water motion as well as water surface elevation. For the purposes of this study, the solution of the water surface (Equation 2-23) was used while the solutions for water velocity were ignored. The solution of water level largely depended on the parameters  $\kappa$  and  $\delta$ .

Values for  $\kappa$  and  $\delta$  were estimated based on the length of the idealized basin (32 km) and a constant approximate depth of the idealized basin (5 m). The bathymetry for the idealized basin was approximated using non-dimensional values shown in Equations 4-1 and 4-2 and the ideal bathymetry is shown in Figure 4-1.

$$h = 0.01 + 0.99(1 - y^4) \quad (4-1)$$

$$y = -1:0.1:1 \quad (4-2)$$

A plot of the best values for  $\kappa$  and  $\delta$  is shown in Figure 4-2. This plot shows the amount of error associated with the combination of values.  $\kappa$  values ranged from 0.25 to 0.85 and  $\delta$  values ranged from 0 to 1.8. The area of best fit found  $\kappa$  to be approximately 0.5 to 0.6 and  $\delta$  values to be approximately 1.2 to 1.3.

To compare these results with the CEOF results, three of the best fit values for  $\kappa$  and  $\delta$  were used to find the corresponding free surface elevation (Equation 2-23) from the analytical model. The  $\delta$  values were 1.3, 1.24, and 1.2 and the associated  $\kappa$  values were 0.5, 0.53, and 0.6 respectively. The amplitude of  $N$  from the chosen values of  $\kappa$

and  $\delta$  were found and plotted with Mode 1 (Figure 4-3). Each of the three model approximations did not account for the attenuation of the amplitude between Old Port Tampa and McKay Bay. Therefore, the best fit for all four stations was found to be  $\kappa = 0.53$  and  $\delta = 1.24$  with an error of 1.8%. However, a closer match can be seen from Figure 4-3 for the first three stations. I believe the model cannot predict this attenuation due to the real geometry of the Bay. In the idealized basin, the bay is rectangular with each port along the bay forming a line down the bay. In reality, McKay Bay is protected from the incoming wave action from the ocean. For this reason, the model was successful in predicting the subtidal wave propagation for the first three ports but doesn't apply to the protected port.

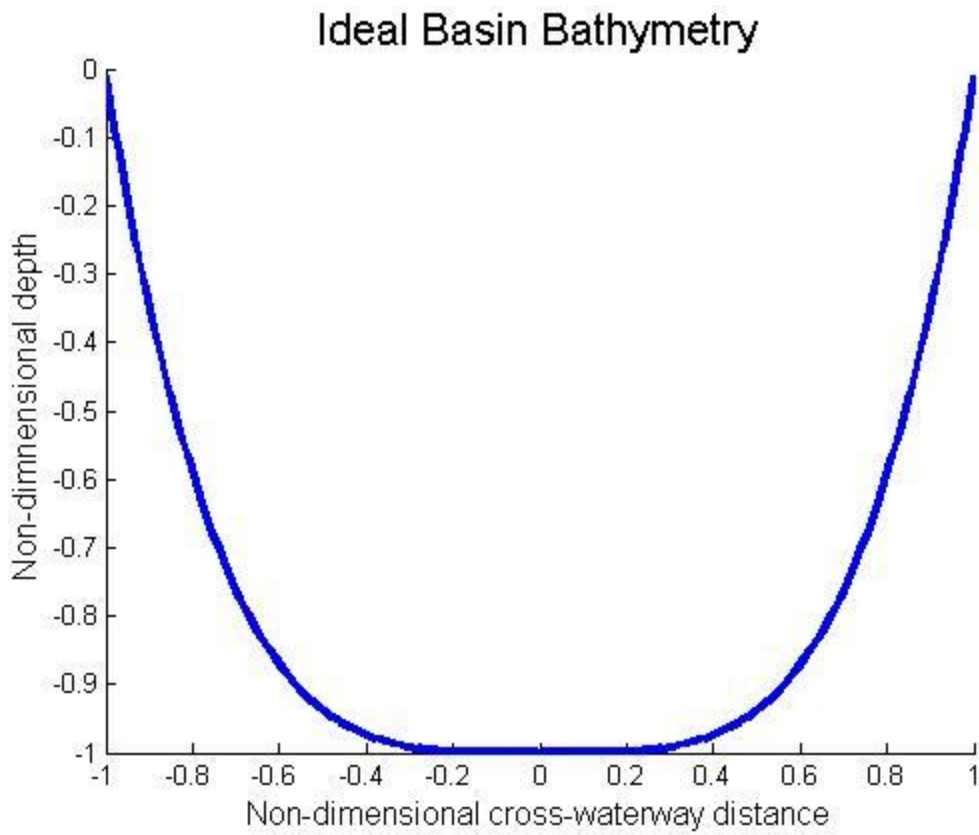


Figure 4-1. Ideal basin bathymetry

RMSe as a function of  $\delta$  and  $\kappa$

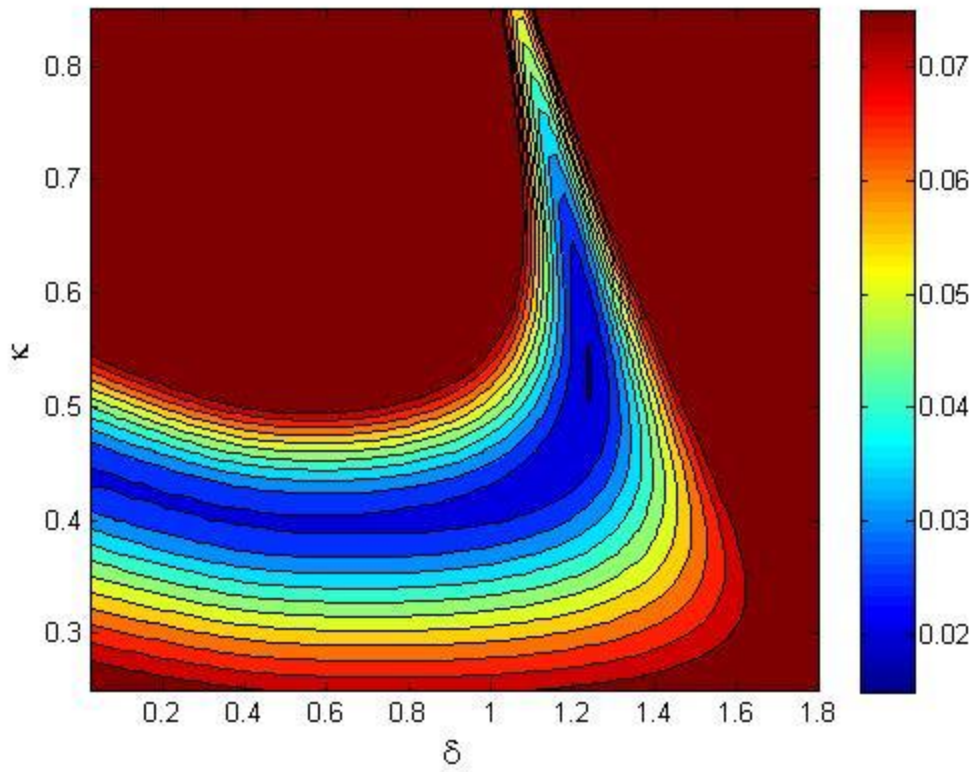


Figure 4-2. RMSe of various  $\kappa$  and  $\delta$  values

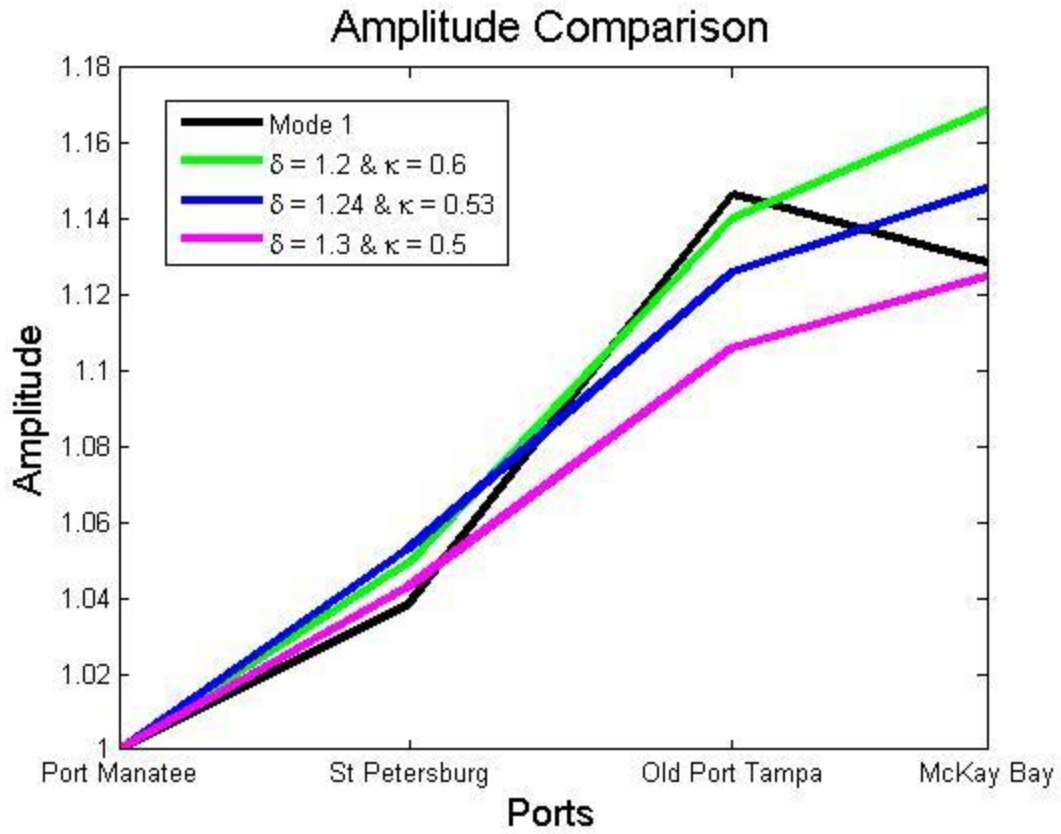


Figure 4-3. Amplitude comparison between Mode 1 and values from the model

## CHAPTER 5 CONCLUSION

The subtidal water levels in Tampa showed an extreme maximum in late April in 2012. This maximum pulse coincided with a minimum pressure. Therefore, the maximum subtidal water level is due to meteorological reasons. In addition, a wavelet transform of the subtidal water levels showed a peak in the power spectrum during that same time period. This peak held a period of 4-16 days, which is associated with the maximum subtidal water level. The propagation of the subtidal pulses was explored through the use of CEOF analysis and an appropriate analytical model. The CEOFs showed an amplification of the subtidal signal with a 4% increase between Port Manatee and St Petersburg, 11% increase between St Petersburg and Old Port Tampa. The 2% decrease of the signal between Old Port Tampa and McKay Bay resulted from the geometry of the bay such that McKay Bay is protected from the incoming wave action. More stations within the main channel of the bay would give a better indication of the subtidal wave behavior within the bay. The inclusion of the McKay Bay caused extraneous results. The model was used to compare to the statistical analysis by finding  $\kappa$  and  $\delta$  values that best fit for Tampa Bay. The best fit value of  $\kappa = 0.53$  explains that the basin of study is approximately one tenth of the wavelength of the subtidal wave. The best fit value of  $\delta = 1.24$  means the entire water column experiences frictional effects.

## LIST OF REFERENCES

- Galperin, B., A. Blumberg and R. Weisberg (1991), A time-dependent three-dimensional model of circulation in Tampa Bay, paper presented at Proceedings of the Tampa Bay Area Scientific Information Symposium.
- Goodwin, C. (1987), Tidal-flow, circulation, and flushing changes caused by dredge and fill in Tampa Bay, Florida, US Government Printing Office.
- Lewis, R.R.I., and E.D. Estevez (1988), The ecology of Tampa Bay, Florida: an estuarine profile, U.S Fish Wildlife Service Biological Report., 85(7.18), 132.
- Mellor, G. (1996), Introduction to Physical Oceanography, American Institute of Physics.
- Sheng, Y., V. Alymov and V. Paramygin (2010), Simulation of storm surge, wave, currents, and inundation in the Outer Banks and Chesapeake Bay during Hurricane Isabel in 2003: The importance of waves, Journal of Geophysical Research., 115(C04008), 1-27, doi: 10.1029/2009JC00.
- Shi, J., M. Luther and S. Meyers (2006), Modelling of wind wave-induced bottom processes during the slack water periods in Tampa Bay, Florida., International Journal for Numerical Methods in Fluids., 52, 1277-1292, doi: 10.1002/flid.1377.
- Snedden, G., J. Cable and W. Wiseman (2007), Subtidal Sea Level Variability in a Shallow Mississippi River Deltaic Estuary, Louisiana, Estuaries and Coasts., 30(5), 802-812.
- Tebaldi, C., B. Strauss and C. Zervas (2012), Modelling sea level rise impacts on storm surges along US coasts, Environmental Research Letters., 7(1).
- Torrence, C., and G.P. Compo (1998), A practical guide to wavelet analysis, Bulletin of the American Meteorological Society., 79, 61-78.
- Weisberg, R., and L. Zheng (2006), Circulation of Tampa Bay driven by buoyancy, tides, and winds, as simulated using a finite volume coastal ocean model, Journal of Geophysical Research., 111, doi: 10.1029/2005JC003067.
- Weisberg, R., and L. Zheng (2008), Hurricane storm surge simulations comparing three-dimensional with two-dimensional formulations based on an Ivan-like storm over the Tampa Bay, Florida region, Journal of Geophysical Research., 113(C12001).
- Winant, C. (2007), Three-dimensional tidal flow in an elongated, rotating basin, Journal of Physical Oceanography., 37, 2345-2362.

## BIOGRAPHICAL SKETCH

Kirsten started her journey to coastal engineering by first traveling to Boca Raton in fall 2007. There, she started her undergraduate program in ocean engineering at Florida Atlantic University. Through her time at FAU, she was involved in Society of Women Engineers (becoming Vice President and President in successive years) and Engineering Student Council. She also spent a majority of her undergraduate career tutoring others in Calculus with Supplemental Instruction and the Math Learning Center at FAU. Upon graduation in 2012, Kirsten immediately started working on her Master of Science in coastal engineering at University of Florida. She graduated in May 2014.